Proceedings of Global Power and Propulsion Society
ISSN-Nr: 2504-4400
GPPS Xi'an21
18th–20th October, 2021

www.gpps.global

GPPS-TC-2021-328

Propeller Design and Performance Evaluation with Partially Prescribed Velocity Distribution

Sebastian Lück, Jan Göing, Tim Wittmann
Bastian Kirsch, Leroy Benjamin, Jens Friedrichs
Institute of Jet Propulsion and Turbomachinery
Technische Universität Braunschweig
s.lueck@ifas.tu-braunschweig.de
Brauschweig, Germany

ABSTRACT

This research aims to provide an iterative propeller design approach for distributed electric propulsion (eDEP) systems with the example of improved cooling characteristics. This is achieved due to increased outflow velocity near the hub where a heat exchanger is placed. For this purpose, the in-house tool RAPID (Research Algorithm for Propeller Identification and Design) is presented. Its propeller design algorithm is based on the Blade Element Momentum Theory with Betz' optimal displacement velocity ratio. Patterson's approach for prescribed axial velocities is used for the modified cooling characteristics. The propeller design with modified near-root velocity distribution is presented for an eDEP propulsion unit of a 50 pax regional aircraft class. In the following, the on- and off-design performance of the design is shown. Subsequently, the improved cooling performance is discussed by applying an analytical fin heat exchanger model in the propeller outflow. It can be shown that the modifications result in a significant reduction in the required heat exchanger size of up to 3.86%. At the same time, the impact on propeller efficiency remains below 0.44% at take-off while it inreases up to -2.41% at cruise.

INTRODUCTION

The conversion of aviation propulsion from aero gas turbines to electrically driven systems requires a revision of the design concepts used in the development stages of future propulsion units. The main advantages of electric propulsion are high efficiencies over a broad operating range, the possibility to use distributed propulsion due to the uncoupling of energy source and the propulsor and a variety of possible power sources such as batteries or fuel cells. Thorough investigations on the placement and synergetical interaction of DEP systems are given by Borer et al. (2017). Electric propulsion is currently only conceivable for short-haul regional aircraft. Their cruising speed and altitude are in a range where propeller-driven aircraft have their main advantages. The degrees of freedom gained have to be fed back into the design process of the drivetrain components such as electric motor, power electronics and the propeller. The design of a propulsion unit including propeller, electric motor and power electronics is the main focus of the EProRef (Electric Propulsors for Regional aircraft) project. The project goals of the consortium are the investigation and development of a distributed electric propulsion unit including propeller, electric motor and power electronics. The requirements are obtained from a regional aircraft for 50 PAX and a range of 1000 km. These requirements represent the ATR42-500 aircraft which is powered by two Pratt & Whitney P127E turboprop engines rated at $P \approx 1790$ kW continuous power. By replacing the engines with an electric powerplant of the same power, electric losses would increase drastically and the use of superconductors become mandatory. To avoid this, a distributed electric propulsion approach (eDEP) is used in EProReF. A discussion and an overview on onboard electronics of more-electric and all-electric aircraft are given by Schefer et al. (2020) and examples for compact mobile applications of drive inverters can be found in Langmaack et al. (2019). Additionally, initial studies have to be carried out to determine the number, orientation and position of the propulsors with respect to the wing which are suited best for the reference aircraft. These

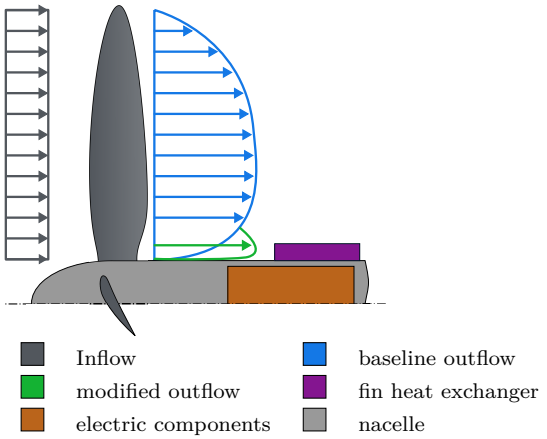

Figure 1 Schematic of propulsor setup with baseline and modified outflow velocity distribution in front of downstream heat exchanger.

Table 1 Fullscale and scaled DEP propeller boundary conditions.

		ATR42-500	DEP 6	scaled DEP 6
d_{Prop}	in m	3.96	1.0	0.8
d_{hub}	in m	0.65	0.40	0.33
N	in min^{-1}	1212	4800	6000
T_{EoF}	in N	19800	3300	2112
Ma_{tip}		0.732		
J		0.713		

Table 2 Scaled DEP 6 design requirements at 4 operating points.

		Take-Off	HHA	ToC	Cruise
T_{req}	in N	2112	2112	352	277
V_{inf}	in m/s	57	57	118	128
h	in m	0	3048	6000	6000
P_{loss}	in kW	14	14	2.9	2.3

simulations will be carried out using CFD with the actuator disk approach as a reduced order model to substitute the propeller (Raichle et al. (2007)) in the scope of EProRef. Subsequently, propellers are designed using the in-house tool RAPID (Research Algorithm for Propeller Identification and Design) which is described later in this paper. Since cooling of electric motors and power electronics at low temperature gradients can be an issue, especially at harsh hot day and high altitude conditions at take-off, further investigations regarding the cooling concepts are scheduled and a design approach is presented in this study.

PROPELLER DESIGN REQUIREMENTS

The design of the propeller for the present case is oriented towards the most critical point of the mission, which is the end of field with one engine inoperative (EoF) scenario. At this point of the project, no considerations regarding redundancy and possible failures have been conducted. Therefore, the required thrust at this mission point is adopted from the reference aircraft. The derived requirements are presented in tab. 1. In order to accommodate the propulsion unit in the test section of a wind tunnel and to minimise side wall effects, the propeller diameter d_{prop} has to be scaled to a diameter of $d_{prop} = 0.8$ m. This ensures a distance from propeller tip to the side walls of $1 \cdot d$. Scaling is done by keeping the disc loading P/A as well as the rotational speed N constant. The requirements and boundary conditions are given in tab. 2 at the considered operating points: take-off, hot day high altitude take-off (HHA), top of climb (ToC) and cruise. For the current design, a setup of six propulsors (DEP6) per wing will be used as input for the design process. Preliminary studies have shown that a design of the propeller for the cruise operating point leads to designs that can not fulfill the thrust requirement at Eof. In addition to the propeller design, another focus of the project is the cooling system of the propulsion unit. In order to achieve a compact packaging, value is placed on using the propeller slipstream for cooling. A thermal analysis for heat exchangers with a flow inside the nacelle has been conducted by Schnulo et al. (2017) but it requires an extensive internal fluid flow structure. Additionally, the systems presented are in a range of ≈ 15 kW with thermal losses of up to 220 W. These values are far below the aim of EProRef and therefore, further investigation will be conducted. Since the propeller is designed with the optimum condition of Betz, it has a low near-root velocity, resulting in a low cooling potential. One possibility for improvement is to modify the flow in the near-root region. This approach will be presented in this paper by prescribing a velocity distribution in particular areas of the propeller near the root. A schematic drawing is shown in fig. 1. In addition to the homogenous inflow, the outflow velocity distribution is shown. In the near-root region, a fin heat exchanger is placed downstream of the propeller.

After introducing this main concept, this paper aims to investigate the central research question: how can the performance of a local heat exchanger downstream of a propeller in an eDEP setup be improved by manipulating the local propeller design velocity? To do so, and with the scope of the EProRef project presented, the RAPID design process is depicted. Afterwards, the modification of the standard design process by using the approach of Patterson is given. For the subsequent evaluation of the design, a brief introduction of the heat exchanger model and its simplifications are given. In the following, results for propeller design of baseline and modified approach are given during on- and off-design operation based on the BEMT. Finally, heat exchanger performance improvement is discussed.

METHODOLOGY

The superordinate design process for propellers at IFAS is depicted in fig. 2. It starts with the specification of geometrical boundary conditions and thrust or power requirements ①. These are used in the classic methods of the Blade Element Momentum Theory (BEMT) ②.

The propeller design algorithm used herein is the one presented by Adkins and Liebeck (1994). It is based on the work of Glauert (1935) and aims at designing a propeller of optimum efficiency according to the formulation of constant displacement velocity ratio ζ by Betz (1919). This is based on the assumption that the propeller wake has the lowest loss of energy if the vortex sheet moves axially downstream and has the shape of a rigid screw surface. The algorithm has been implemented in MATLAB 2021 for the subsequent propeller design according to the algorithm of Adkins and Liebeck with the optimum Betz criterion. The condition is met by iterating the displacement velocity ratio ζ for the entire span of the propeller blade until a constant ζ is achieved for all blade elements. Supplementary airfoil section data in form of airfoil polars providing lift (C_L) and drag (C_D) is obtained for the requested airfoil at each section using XFOIL (Drela (2013)) with $N_{crit} = 4.5$ and stored in a database. To avoid program errors when leaving the polar range, all polars are extended by scaled NACA0012 polars (Critzos et al. (1955)) to a range of -180° to +180°. Even though realistic designs should not have any operating points outside of the previously generated polar, this approach greatly improves the stability of the iterative process. (Approaches in Literature for 360° polar extension: Morgado et al. (2013) Traub (2016)). The evaluation of the airfoil database is performed using linear interpolation for queried angle of attack α, Re and Ma during the algorithm.

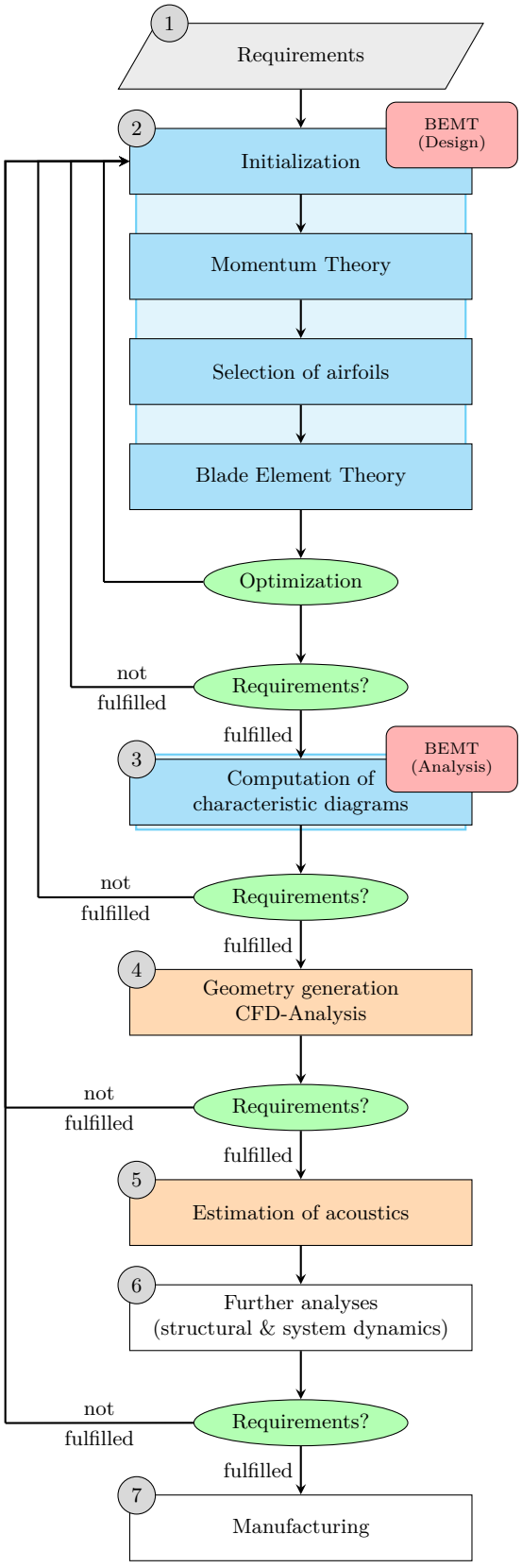

Figure 2 Flowchart of the RAPID propeller design workflow.

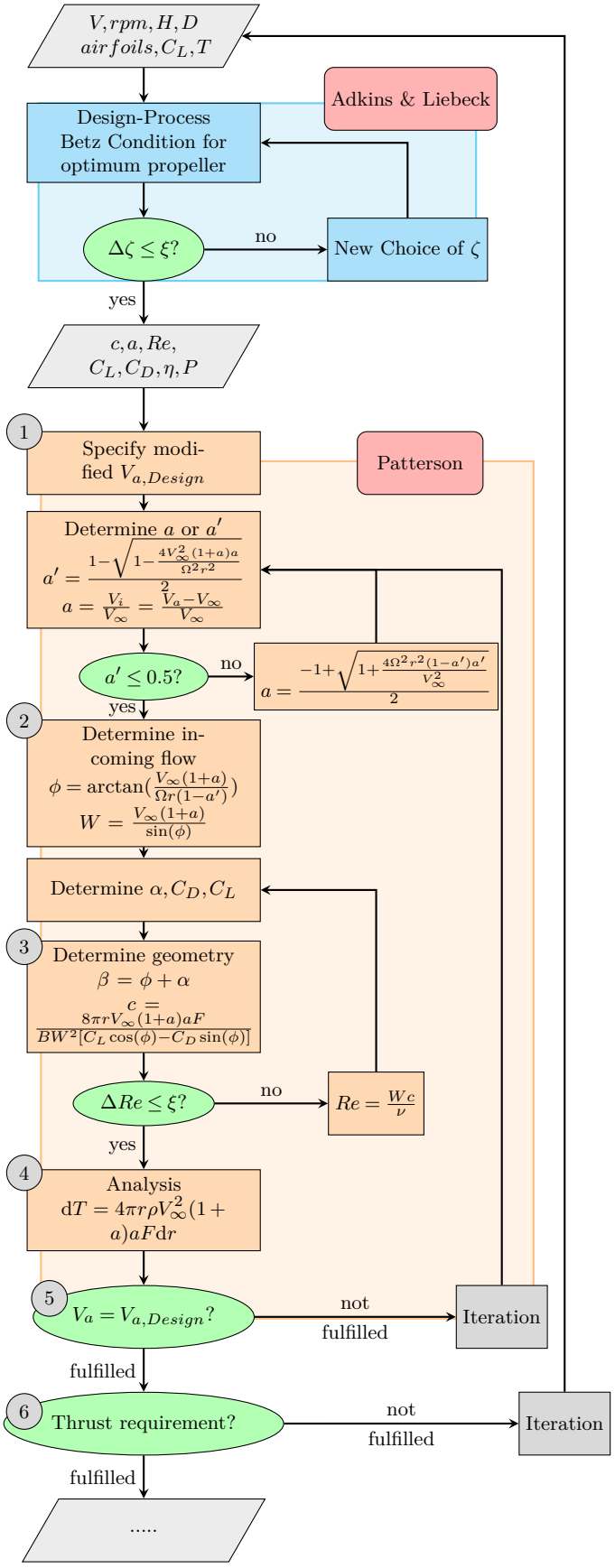

Figure 3 Flowchart of the workflow for modified propeller design.

A subsequently conducted independency study for the propeller of Adkins has shown that for the entire range of Re and Ma occurring along the propeller blade, a grid of at least 100 polars on an evenly spaced grid of 10x10 Re x Ma should be used to avoid additional discretization uncertainties.To evaluate the propeller of the generated propeller design, the results of the aforementioned design process (chord length c, twist angle β, airfoil, radial position) and boundary conditions from tab. 2 are used as inputs for the calculation of off-design operating points ③. Performance maps for a 3D operating space over a range of advance ratios J, pitch angles Φ and altitudes h are calculated subsequently by iterating the axial and rotational velocity induction factors a and a'. While various works deal with solution approaches for the BEMT (Ledoux et al. (2020), Liu and Janajreh (2012), Winarto (2004)), a conventional iteration scheme with an under-relaxation factor ω is used: $a_{i+1} = a_i + \omega(a_{i+1} - a_i)$. As suggested by Filippone (2012) and Maheri et al. (n.d.), a factor of $\omega = 0.5$ should be used while exceeding 0.56 will lead to extensive oscillations of the solution. During the solution process in this work, it was found that the best compromise between convergence performance and speed is achieved with an under-relaxation factor of $\omega = 0.01$. This is particularly necessary in regions of the polars with large gradients in the off-design. While not relevant for the propeller design, stall delay models by Dumitrescu and Cardos (2007), Snel et al. (1993), Gur and Rosen (2005) and Corrigan/Schillings have been implemented. These approaches are specific to propellers or wind turbines and extend the 2D polars by taking into account rotational effects caused by the centrifugal forces. Subsequently, stall will be shifted to higher angles of attack.
In order to validate the implementation of Adkins algorithm, validations have been carried out using the propeller design provided by Adkins as well as that of Park et al. (2018). For both designs, airfoil section data as well as all operational point data is available. Design points for both propellers can be matched in terms of thrust and power coefficient as well as efficiency. During the validation the advantage of using 360° polars becomes evident: even above stall, RAPID is able to iterate operating points robustly without troubleshooting due to exceeding the polar range. However, the significance of such operating points is limited because a propeller would usually not be operated above stall. Furthermore, the momentum theory is not valid for flight velocity of V_{inf}=0 m/s. Subsequently, equations for static thrust can be used (Gudmundsson (2014)). In addition to the validation with literature, the Adkins propeller has been redesigned using JavaProp by Hepperle (2020).

Table 3 Heat exchanger dimensions

		$\cdot R_{hub}(\%)$
fin height	h_{fin}	17.93
fin width	t_{fin}	2.25
gap width	t_{gap}	4.6
no. of fins	(-)	100

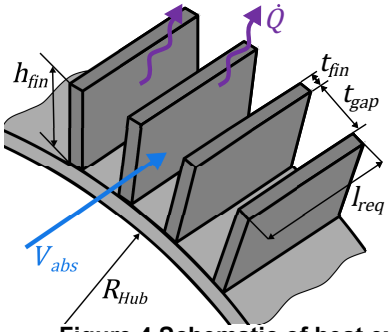

Figure 4 Schematic of heat exchanger.

The results are in agreement throughout a realistic operating range. Subsequently, a 3D geometry can be generated using standard CAD software and used for CFD analysis ④. In the scope of EProRef, DLR Tau-Code is to be used for 2D actuator disk (AD) CFD in order to determine the propeller location in relation to the wing. 3D high fidelity RANS and uRANS CFD will be used for detailed aerodynamic analysis such as propeller wake-wing interaction. The 3D CFD flow field is then used to determine acoustic characteristics using DLR PIANO code ⑤. Additionally, structural (FEM) and dynamic investigations (FDM) can be conducted using finite element method (FEM)⑥. Ultimately, manufacturing in carbon fibre composite material terminates the propeller design workflow ⑦.

While the previously described workflow gives the overall framework for the propeller design, a different approach is used in order to improve the overall cooling characteristics of the propeller outflow in a downstream heat exchanger. In contrast to the previously described design with minimal induced losses, a different approach is presented by Patterson, Borer and German (2016) with the goal of achieving a uniform axial velocity distribution behind the propeller. The main purpose herein is providing a uniform inflow for the wing of a distributed electric propulsion aircraft (NASA X-57). However, the propellers designed by this approach do not have the objective of thrust generation. Their task is much more the generation of a uniform and amplified axial inflow velocity towards the wing. They are subsequently called high lift propellers since they operate only during take off and landing. Thrust is generated by a set of additional wing tip propellers.
The algorithm proposed by Patterson, Derlaga and Borer (2016) is based on the same overall equations used in Adkins and Liebeck (1994) but instead of iterating a constant ζ, the induced velocity factors are predefined for the high lift propeller configuration. It will now be used to prescribe the outflow's velocity for the near root section of the propeller. This is achieved by inserting the process depicted in fig. 3 into ② in fig. 2.

In the process presented in this paper, the optimum propeller design is coupled with the process by Patterson to achieve an optimum propeller performance according to Betz criterion along most of the span. The section that is altered for cooling performance improvement is modified using Pattersons' approach. In the near root region (r^*_{mod}) where the heat exchanger will be located downstream, V_a is modified to increase the outflow velocity by 10% over the baseline design ①. Other distributions of $V_a(r^*)$ are possible but are not presented for the sake of simplicity. From the initial design, a is used to calculate a'. Subsequently, the corresponding inflow conditions Φ and W can be established ②. From that point, the airfoil angle of attack α, C_L and C_D can be determined by either specifying a design lift coefficient or by iterating for the optimum lift-to-drag ratio ϵ. The coefficients are obtained from the database previously discussed. Since the geometry of the blade is the result of the design, chord length c and blade twist angle β are then calculated ③. Since the Reynolds Number is going to change with every change of the chord c, an inner loop is executed until it has converged to a constant Re. Ultimately, the thrust dT of every blade element of the modified propeller is calculated and integrated to obtain the overall thrust ④. Ultimately, the induced axial velocity in the modified region is compared to $V_{a,Design}$ and $a(r^*_{mod})$ is iterated ⑤.

Since altering the axial velocity leads to an increased thrust, the initial thrust requirement for the optimum design process is iterated using Newton's method ⑥. The new $a(r^*)$ distribution for the unmodified region is taken from the iterated Adkins design while the $V_{a,Design}$ distribution for the modified region is held constant according to the pre-definition for this region. Iteration converges if the thrust of the modified propeller matches the thrust requirement. Convergence is usually achieved after 5 iterations of the loop.

Heat exchanger calculation

The performance of the fin heat exchanger around the circumference of the nacelle downstream of the propeller is estimated using a model for flat gap heat exchange. The calculation workflow is depicted in VDI e. V. (2013). More specific, equations for the Nusselt number Nu in the turbulent regime are obtained from

Gnielinski (1975). The influence of temperature dependency of the gas thermal properties on heat transfer is considered by a correction for gasses $Nu = Nu_m \cdot (T_{air}/T_{wall})^n$ with $n = 0.45$

$$Nu_{turb} = \frac{\frac{\xi \cdot Re \cdot Pr}{8}}{1 + 12.7\sqrt{\frac{\xi}{8}}\left(Pr^{2/3} - 1\right)} \left[1 + \left(\frac{d_h}{l}\right)^{2/3}\right] \cdot \left(\frac{T_{air}}{T_{wall}}\right)^{0.45} \tag{1}$$

where

$$\xi = \left(1.8 \cdot log_{10}(Re) - 1.5\right)^{-2} \tag{2}$$

The main simplifications that were made are the assumption of a uniform inflow velocity perpendicular to the front face of the heat exchanger as well as a flow parallel to the wall. The inflow velocity is calculated by averaging the propeller outflow velocity over the height of the fins. At the present state, no upstream effects like blockage or pressure perturbation due to the cooling fins are fed back into the design process. Furthermore, recirculating cooling liquid is assumed to achieve a uniform wall temperature of $T_{wall} = 331.15$ K for the entire length of the heat exchanger and mass flow continuity is assumed. The geometrical boundary conditions of the heat exchanger are given in tab. 3 as multiples of the hub radius R_{Hub}. The resulting Reynolds number in the gap related to the hydraulic diameter is in the range of $6 \cdot 10^4 < Re < 1 \cdot 10^5$. Heat is discharged from the electric components at an estimated rate of 14 kW for a system power of 200 kW, electric motor efficiency of $\eta = 96\%$ and power electronics efficiency of $\eta = 97\%$. Other losses are neglected and heat transfer outside the scope of the fin heat exchanger is assumed as ideal. Subsequently, the required length l_{fin} is calculated to ensure the dissipation of all losses generated by motor and power electronics.

PROPELLER DESIGN AND PERFORMANCE RESULTS

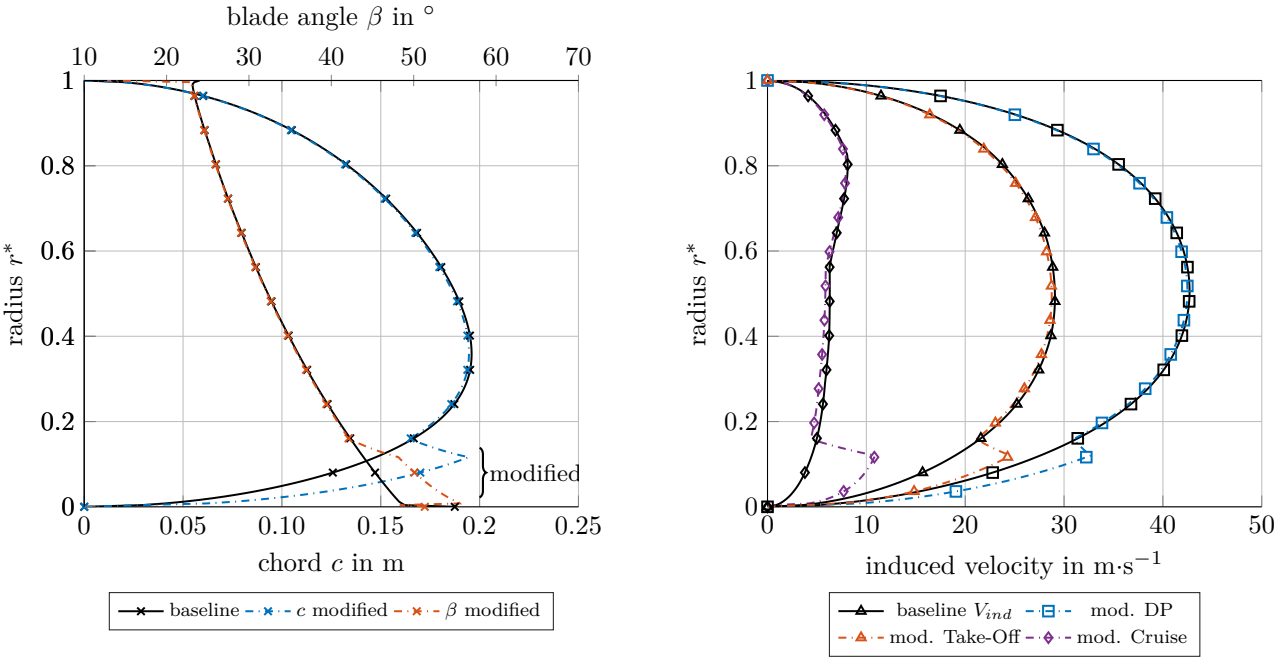

(a) Blade chord length c and angle β along blade span r^*

(b) Induced velocity V_{ind} at the propeller plane

Figure 5 Design results.

For simplicity, the FX63-100 airfoil with a constant $C_L = 0.8$ along the radius was used as design input. The Prandtl tip and root vortex factor formulation is applied to account for losses caused by the vortex system within the mommentum equation. The prescribed velocity in the near-root area over the height of the heat exchanger was increased by 10% compared to the baseline design. A larger increase of the axial velocity can not be achieved for the highly loaded propeller without exceeding the physical limit of $a' = 0.5$ which is almost reached by the baseline design already. In the proximity, a transition to baseline velocity over 10 blade elements is enforced. Fig. 5(a) shows the resulting geometry of the modified propeller design. The modified region clearly stands out with an increase in chord length by up to 51% and 15% in blade angle compared to the baseline geometry of

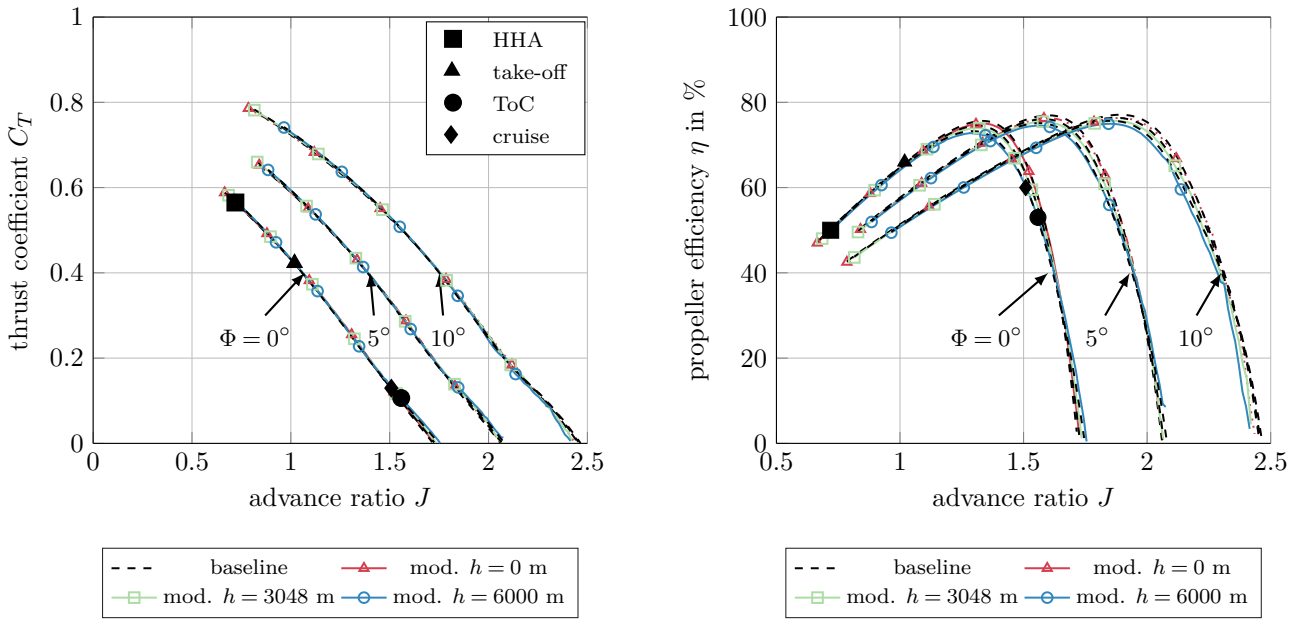

(a) Thrust coefficient C_T over advance ratio J

(b) Efficiency η_{prop} over advance ratio J

Figure 6 Propeller design performance for three pitch angles Φ and altitudes h from tab. 2.

equivalent design thrust. The corresponding velocity distributions behind the propeller are depicted in fig. 5(b) for operating points from tab. 2. The modified prescribed velocity distribution in the wake near the root area is clearly visible between $0 < r^* < 0.116$. While the impact at the design point is obvious, the modification leads to a further increase of the velocity at sea level take-off up to 36% and up to a factor of 3.5 at cruise.

In the next step, the design is evaluated for further off-design conditions at altitudes labeled in tab. 2. In addition, a series of positive pitch angles Φ is shown and the operating points are highlighted in fig. 6. While not shown in fig. 6, operating points of the baseline design are overall located at higher efficiencies. Fig. 6(a) shows, that all operating points can be reached by the current design and differences between baseline and modified design are negligible. As seen in fig. 6(b) all operating points are either below or above the J of optimum efficiency. It has to be investigated, whether fixed pitched operation strategy is feasible for electric distributed propulsion. In contrast to gas turbine driven propulsion, the electric motor provides high efficiencies over a broad operating range. The trade-off in mechanical complexity and weight against propeller efficiency needs to be addressed in the future.

The reduction in heat exchanger length is presented in fig. 7. The modified outflow leads to an average reduction in heat exchanger length of up to 3.86% at the critical HHA operating point. In contrast, only 0.44% of efficiency degradation are predicted by the BEMT for this scenario. Almost the same result is predicted at sea level take-off. This gain however comes with a significant penalty in cruise efficiency of up to -2.14%. If one would use these results for the heat exchanger design, a length of $2.65 \cdot R_{Hub}$ or 42.53 cm would be required. The HHA operating point is of most interest here, because cooling is challenging due to low density and temperature gradients. The required length is almost 2.5 times the length required at sea level and should therefore be used as the critical reference in the future.

CONCLUSIONS AND OUTLOOK

A design process for propellers with extended capabilities for predefined axial velocity has been presented in this paper. The workflow of the required tools in the overall design process of RAPID has been pointed out. For the detailed BEMT workflow, two approaches known from established literature were merged. Most important boundary conditions for the algorithm have been laid out and are believed to aid the general implementation approach for such project. The main goal of the newly developed process is to answer the question on how the performance of a local heat exchanger downstream of the propeller can be improved by manipulating the design velocity distribution. An application case in form of the EProRef project for electrically driven regional aircraft has been introduced and will be pursued in the following years. Based on the boundary conditions, an application case for the model has been generated and a design study was conducted. The axial induced velocity near the blade root was increased by 10% compared to a minimum induced loss design while thrust was held constant.

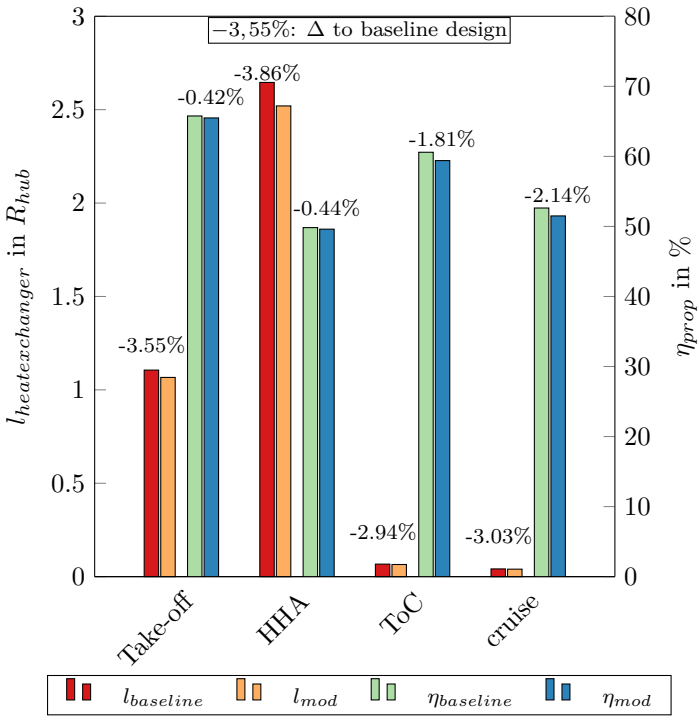

Figure 7 Design modification impact on heat exchanger length $l_{heatexchanger}$ (left axis) and relative change compared to baseline. Propeller efficiency η_{prop} (right axis) and absolute change compared to baseline for the operating points under investigation.

In combination with a fin heat exchanger, which is be placed on the outside of the nacelle, the performace of the design has been evaluated. By modifying the propeller at the near-root region over the height of the heat exchanger, a decrease in required length of up to 3.86% has been calculated. While the penalty on performance at take-off and HHA is rather low, a substantial decrease in propeller efficiency by up to 2.14% is predicted at the cruise operating point. Furthermore, a slight shift of operating points towards higher advance ratios can be detected.

The aim of this work was the preliminary investigation of the cooling interaction between propeller and electric motor. Especially high blade loading in the one engine inoperative scenario has to be reviewed with respect to regulatory requirements and the reliability of electric machines compared to gas turbines. A loss of power for an entire wing seems unlikely. It is emphasized that lower blade loading will enable higher increases of the modified-to-unmodified velocity ratio near the root without reaching unphysical dimensions. Subsequently, for smaller electric motors with less losses, modifications of the cooling system can become more significant. Furthermore, the process of airfoil selection for distinct blade elements needs to be carried out, taking into account aerodynamics as well as structural aspects and manufacturing. Subsequently, 3D CFD simulations of the entire propulsion unit including heat exchangers have to verify if the approach meets real world performance requirements (see fig. 2 ④). Especially the shape of the prescribed velocity field has to be studied in further detail. The authors are aware of the fact that a sawtooth chord length distribution near the hub might cause negative effects on the three dimensional flow. Additionally, the shape of the downstream heat exchanger's fins could be changed to that of a aerodynamic stator for optimized pressure recovery. From the 3D flow field, the acoustic footprint of the design can be assessed (fig. 2 ⑤). Additionaly, modal analysis using FEM and transient dynamic system performance simulations using FDM (e.g. Goeing et al. (2020)) are going to be carried out to predict the drivetrain performance. Furthermore a trade-off in weight and mechanical complexity vs. propeller efficiency needs to be adressed for the use of variable RPM systems compared to constant speed gas turbines. It has to be established whether the omission of a variable pitch system can have a positive overall impact on performance. Finally, wind tunnel tests of the developed propulsion unit are planned for validation of the project.

NOMENCLATURE

RAPID	Research Algorithm for Propeller Identification and Design
BEMT	blade element momentum theory
DP	design point
(e)DEP	(electric) distributed electric propulsion
EoF	end of field
FDM	finite difference method
FEM	finite element method
HHA	hot day high altitude
PTF	Propulsor Test Facility
(u)RANS	(unsteady) Reynolds averaged Navier Stokes
ToC	top of climb

α	angle of attack
a, a'	axial and rotational induction factor
β	blad twist angle
c	chord length
$C_T = T/(\rho \cdot N^2 \cdot d^4)$	thrust coefficient
C_L, C_D	lift and drag coefficient
d, d_h	diameter and hydraulic diameter
η	efficiency
$\epsilon = C_L/C_D$	lift-to-drag ratio
F	loss factor
h	altitude
h_{fin}	fin height
$J = V/(N \cdot d)$	advance ratio
l	heat exchanger length
$modified$	mod
N	rotational speed
N_{crit}	transition criterion (XFOIL)
Ω	angular velocity
P	power
$prop$	propeller
r, $r^* = (r - r_{hub})/(r_{tip} - r_{hub})$	radius or nondimensional radius
req	required
t_{gap}, t_{fin}	gap and fin width
dT, T	blade element and overall thrust
T_{wall}, T_{air}	wall or air temperature
V_a, V_i, V_{inf}	axial, induced and inflow velocity
ν	viscosity
Nu, Pr, Re	Nusselt, Prandtl, Reynolds number
Φ	flow angle
W	total velocity
ζ	displacement velocity ratio

ACKNOWLEDGMENTS

The authors gratefully acknowledge the works of Johanna Ehlert and Patrick Meyer for the work during their student thesis. Furthermore, the authors thank Simon Wolfstädter and Thomas Reis from Oswald Elektromotoren GmbH as well as Robert Rohn and Dirk Fischer from IMAB for their support and helpful discussions. The authors gratefully acknowledge the financial support of the German Federal Ministry of Transport and Digital Infrastructure for the EProRef project (Grant No. 20M1906B) as well as the funding by the Deutsche Forschungsgemeinschaft (DFG, German Research Foundation) under Germany's Excellence Strategy – EXC 2163/1 – Sustainable and Energy Efficient Aviation – Project-ID 390881007.

ORCID ID

Sebastian Lück orcid.org/0000-0003-1696-1300

Jan Göing orcid.org/0000-0002-1279-1933

Tim Wittmann orcid.org/0000-0001-9948-2860

References

Adkins, C. N. and Liebeck, R. H. (1994). Design of optimum propellers, *Journal of Propulsion and Power* **10**(5): 676–682.

Betz, A. (1919). Schraubenpropeller mit geringstem Energieverlust. Mit einem Zusatz von l. Prandtl, *Nachrichten von der Gesellschaft der Wissenschaften zu Göttingen, Mathematisch-Physikalische Klasse* **1919**: 193–217.

Borer, N. K., Derlaga, J. M., Deere, K. A., Carter, M. B., Viken, S., Patterson, M. D., Litherland, B. and Stoll, A. (2017). Comparison of Aero-Propulsive Performance Predictions for Distributed Propulsion Configurations, *55th AIAA Aerospace Sciences Meeting*, American Institute of Aeronautics and Astronautics, Grapevine, Texas.

Critzos, C. C., Heyson, H. H. and Boswinkle Jr, R. W. (1955). Aerodynamic characteristics of NACA 0012 airfoil section at angles of attack from 0 deg to 180 deg, *Technical report*, NATIONAL AERONAUTICS AND SPACE ADMINISTRATION WASHINGTON DC.

Drela, M. (2013). XFOIL: Subsonic Airfoil Development System, v6.99. Available online.

Dumitrescu, H. and Cardos, V. (2007). A stall-delay model for rotating blades, *PAMM* **7**(1): 4100003–4100004.

Filippone, A. (2012). *Advanced Aircraft Flight Performance*, Cambridge University Press, Cambridge.

Glauert, H. (1935). Airplane Propellers, *in* W. F. Durand (ed.), *Aerodynamic Theory: A General Review of Progress Under a Grant of the Guggenheim Fund for the Promotion of Aeronautics*, Springer, Berlin, Heidelberg, pp. 169–360.

Gnielinski, v. V. (1975). Neue Gleichungen für den Wärme- und den Stoffübergang in turbulent durchströmten Rohren und Kanälen, p. 9.

Goeing, J., Seehausen, H., Pak, V., Lueck, S., Seume, J. R. and Friedrichs, J. (2020). Influence of combined compressor and turbine deterioration on the overall performance of a jet engine using RANS simulation and Pseudo Bond Graph approach, *Journal of the Global Power and Propulsion Society* **4**: 296–308.

Gudmundsson, S. (2014). The Anatomy of the Propeller, *General Aviation Aircraft Design*, Elsevier, pp. 581–659.

Gur, O. and Rosen, A. (2005). Propeller Performance at Low Advance Ratio, *Journal of Aircraft* **42**(2): 435–441.

Hepperle, M. (2020). JavaProp - Design and Analysis of Propellers v21.05.2018.

Langmaack, N., Tareilus, G. and Henke, M. (2019). Modular Power Electronics for Electric Vehicles and Aviation Applications, *2019 IEEE 13th International Conference on Power Electronics and Drive Systems (PEDS)*, IEEE, Toulouse, France, pp. 1–5.
URL: *https://ieeexplore.ieee.org/document/8998936/*

Ledoux, J., Riffo, S. and Salomon, J. (2020). Analysis of the Blade Element Momentum Theory, *arXiv:2004.11100 [cs, math]* .

Liu, S. and Janajreh, I. (2012). Development and application of an improved blade element momentum method model on horizontal axis wind turbines, *International Journal of Energy and Environmental Engineering* **3**(1): 30.

Maheri, A., Noroozi, S., Toomer, C. and Vinney, J. (n.d.). Damping the fluctuating behaviour and improving the convergence rate of the axial induction factor in the BEMT- based rotor aerodynamic codes, p. 4.

Morgado, J. P., Silvestre, M. A. and Pascoa, J. (2013). Full Range Airfoil Polars for Propeller Blade Element Momentum Analysis, *2013 International Powered Lift Conference*, American Institute of Aeronautics and Astronautics, Los Angeles, CA.

Park, D., Lee, Y., Cho, T. and Kim, C. (2018). Design and Performance Evaluation of Propeller for Solar-Powered High-Altitude Long-Endurance Unmanned Aerial Vehicle, *International Journal of Aerospace Engineering* **2018**: 1–23.

Patterson, M. D., Borer, N. K. and German, B. (2016). A Simple Method for High-Lift Propeller Conceptual Design, *54th AIAA Aerospace Sciences Meeting*, American Institute of Aeronautics and Astronautics, San Diego, California, USA.

Patterson, M. D., Derlaga, J. M. and Borer, N. K. (2016). High-Lift Propeller System Configuration Selection for NASA's SCEPTOR Distributed Electric Propulsion Flight Demonstrator, *16th AIAA Aviation Technology, Integration, and Operations Conference*, American Institute of Aeronautics and Astronautics, Washington, D.C.

Raichle, A., Melber-Wilkending, S. and Himisch, J. (2007). A new actuator disk model for the tau code and application to a sailplaine with a folding engine, *New Results in Numerical and Experimental Fluid Mechanics VI*, Springer, pp. 52–61.

Schefer, H., Fauth, L., Kopp, T. H., Mallwitz, R., Friebe, J. and Kurrat, M. (2020). Discussion on Electric Power Supply Systems for All Electric Aircraft, *IEEE Access* **8**: 84188–84216.
URL: *https://ieeexplore.ieee.org/document/9086510/*

Schnulo, S. L., Chin, J., Smith, A. and Paul-Dubois-Taine, A. (2017). Steady State Thermal Analyses of SCEPTOR X-57 Wingtip Propulsion, *17th AIAA Aviation Technology, Integration, and Operations Conference*, American Institute of Aeronautics and Astronautics, Denver, Colorado.

Snel, H., Houwink, R., Bosschers, J., Piers, W. J., Van Bussel, G. J. W. and Bruining, A. (1993). Sectional prediction of s-D effects for stalled flow on rotating blades and comparison with measurements.

Traub, L. (2016). Simplified propeller analysis and design including effects of stall, *The Aeronautical Journal* **120**(1227): 796–818.

VDI e. V. (ed.) (2013). *VDI-Wärmeatlas*, Springer Berlin Heidelberg, Berlin, Heidelberg.

Winarto, H. (2004). Bemt algorithm for the prediction of the performance of arbitrary propellers, *Centre of Expertise in Aerodynamic Loads*, number 1, p. 46.